

Effects of CeO₂ Content and Particle Size on the Interdiffusion Between an Aluminide Coating and Underlying Substrate at High Temperature

Tan Xiaoxiao, Sun Dan

Shanghai University of Engineering Science, Shanghai 201620, China

Abstract: The δ -Ni₂Al₃/Ni coating systems with different CeO₂ contents and particle sizes were specially prepared by partially aluminizing the Ni films containing ~0 wt%, ~1 wt%, ~2 wt% and ~3 wt% nanometer CeO₂ (15~30 nm) and ~1 wt% micrometer CeO₂ (5 μ m). The effects of CeO₂ content and particle size on the interdiffusion between the aluminide coating and underlying substrate were investigated by annealing in vacuum at 1000 °C. The results show that the addition of nanometer CeO₂ into the δ -Ni₂Al₃/Ni coating system could mitigate the interdiffusion between the aluminide coating and underlying substrate and the blocking effect can be significantly improved with the increase of the CeO₂ content. However, the addition of micrometer CeO₂ into the coating system has little influence on the degradation of the aluminide coating. This is intrinsically correlated with the fact that the CeO₂ content and particle size would influence the formation of the CeO₂-rich layer at aluminide/Ni film interface acting as a diffusion barrier between the aluminide coating and substrate.

Key words: aluminide coating; annealing; diffusion barrier; oxide dispersion; interdiffusion

The reactive elements (RE) modified aluminide coatings have been widely used as standalone oxidation resistance coatings or bond coatings in thermal barrier coatings (TBCs) to protect the superalloy components of gas turbines^[1,2]. Extensive researches have reported that the high temperature oxidation performance of the aluminide coatings could be obviously improved by the addition of a small amount of RE, such as Y, Hf, Zr and Ce (or their oxides)^[3-5]. However, protective aluminide coatings on superalloys degrade not only by the loss of Al to form alumina scale, but also by the interdiffusion with the underlying substrate^[6]. Moreover, the inward diffusion of Al would destroy the γ/γ' microstructure of Ni-based superalloys and consequently result in the formation of topologically close packed (TCP) phases and the second reaction zone (SRZ), which could seriously degrade the creep-rupture properties^[7-10].

In order to improve the service life of the coated superalloys, a diffusion barrier (DB) between the coating and the substrate

has been developed for blocking the interdiffusion. A good diffusion barrier should take into account the blocking effect, service life, preparation process and so on. The diffusion barriers currently studied mainly include the metallic, the ceramic and the active DBs. The metallic DBs with good interface bonding are usually developed by a diffusion bond mechanism, which are together with interdiffusion reaction after long-term exposure^[11-13]. By contrast, the ceramic DBs used mainly between MCrAlY coatings and alloys have better ability of blocking elements diffusion^[14,15]. α -Al₂O₃ has attracted the attention of many researchers due to its good combination property of dense structure and unusual phase stability^[16-18]. α -Al₂O₃ can be directly deposited on the surface of Ni-based alloy by chemical vapor deposition. However, the undesired whiskers grow on the surface of the deposited α -Al₂O₃ because of the high contents of Co and Ni in substrate, which is not suitable as a diffusion barrier. To prevent whisker growth, one approach that has been applied is to deposit a

Received date: August 16, 2018

Foundation item: National Natural Science Foundation of China (51501109); Shanghai Municipal Science and Technology Commission Local Colleges and Universities Capacity Construction Project (17030501400)

Corresponding author: Tan Xiaoxiao, Ph. D., Lecturer, Engineering Training Center, School of Materials Engineering, Shanghai University of Engineering Science, Shanghai 201620, P. R. China, Tel: 0086-21-67791247, E-mail: xxtan@sues.edu.cn

Copyright © 2019, Northwest Institute for Nonferrous Metal Research. Published by Science Press. All rights reserved.

layer of TiN between the matrix and the α -Al₂O₃ ceramic layer^[19]. Another approach is to deposit a layer of γ -Al₂O₃ on substrate at lower temperature, which is transformed to α -Al₂O₃ after heating^[20]. However, the thermal shock problems due to the difference of thermal expansion coefficient between the ceramic DBs and alloys may reduce the service life of the coating^[21]. In order to improve the adhesion of ceramic DBs with protective coatings and substrates, the active DBs which react with Al from superalloy substrate and coating are prepared, such as Cr-O-N^[22, 23], Cr-Al-O-N^[24], and yttria partially stabilised zirconia (YSZ) layer^[25]. The DBs act as a reservoir of oxygen and transform into sandwich structured Al-rich oxide/metal/Al-rich oxide during service or post vacuum annealing, which eventually suppress the interdiffusion.

In the previous work, Tan and co-workers^[26] developed a CeO₂ dispersed aluminide coating system by partially aluminizing an electrodeposited Ni film containing CeO₂ nanoparticles. The results showed that the CeO₂-dispersed aluminide coating had excellent degradation resistance both to oxidation and interdiffusion compared with the CeO₂-free aluminide coating. The suppression of the interdiffusion was correlated with the formation of a CeO₂-rich layer between aluminide and Ni acting as a diffusion barrier at high temperature. This coating system with good performance and simple preparation process, accordingly, will be an interesting direction to be explored for the diffusion barrier. In the present work, the effects of CeO₂ content and particle size on the interdiffusion of aluminide coating and underlying substrate were studied based on the earlier work. To exclude the influence of oxidation, the coating system was investigated by vacuum annealing at high temperature.

1 Experiment

Small specimens (15 mm×10 mm×2 mm) used as substrates were cut from pure Ni plates. After being hand-polished using 800# sand paper and then cleaned with alcohol and acetone, the specimens were electrodeposited with a Ni-CeO₂ film from a nickel sulphate bath (150 g/L NiSO₄·6H₂O, 120 g/L C₆H₅Na₃O₇·2H₂O, 12 g/L NaCl, 35 g/L H₃BO₃) loaded with CeO₂ particles. The CeO₂ particles with different sizes (15~30 nm and 5 μ m) were commercial products from Alfa Aesar. The deposited Ni films with different nanometer-CeO₂ contents but similar thickness were available through controlling the particle contents in bath at the same deposition time. The particle contents in bath were 2, 10 and 20 g/L. The Ni film containing CeO₂ in micron size range with similar thickness was also prepared.

The specimens were firstly coated by Ni-CeO₂ coating, and then were aluminized at 620 °C using a conventional halide activate pack-cementation in a powder mixture of Al (particles size: ~75 μ m)+56 wt% Al₂O₃ (~75 μ m)+4 wt% NH₄Cl in an Ar (purity: 99.99%) atmosphere. The earlier works^[5,26] indicated that δ -Ni₂Al₃ was formed by aluminizing Ni film and it grew

inward using the pack-cementation method at 620 °C.

Accordingly, the CeO₂ containing aluminide coating systems with different CeO₂ contents and particle sizes were specially prepared by partially aluminizing the Ni-CeO₂ films. For comparison, another CeO₂-free aluminide coating system of δ -Ni₂Al₃/Ni was also prepared by aluminizing a pure Ni film. The Ni film was electrodeposited from a similar bath above but without CeO₂ particles. Afterwards, the aluminized specimens were annealed for different time at 1000 °C in a vacuum of 1×10⁻⁵ Pa. Scanning electron microscopy (SEM), energy dispersive spectroscopy (EDS), and X-ray diffraction (XRD) were used to investigate the evolution of the microstructure and phase of the aluminide coating annealed for different lengths of time.

2 Results and Discussion

2.1 Microstructures of the as-received coatings

According to the calculation based on EDS analysis results, the deposited Ni films with nanometer-CeO₂ contain ~1 wt%, ~2 wt% and ~3 wt% CeO₂ electrodeposited from the bath added with 2, 10 and 20 g/L CeO₂, respectively. The Ni film containing micrometer CeO₂ contains ~1 wt% CeO₂ particles. Five different aluminide coating systems formed by partially aluminizing the electrodeposited Ni films with and without CeO₂ particles, were denoted coating-1, coating-2, coating-3, coating-4 and coating-5, respectively (as shown in Table 1).

Fig.1 shows the cross-section morphologies of the aluminide coating systems under optical microscope (OM). In the condition, the outer part of the coating is the aluminide coating in its δ phase which has been transformed from the outer Ni film, while the inner part of the coating is the inner Ni film remaining unaluminized as reported in the earlier work^[26]. Accordingly, δ -Ni₂Al₃/Ni coating systems with and without CeO₂ particles are clearly seen in Fig.1. The aluminide coatings are ~20 μ m-thick and the unaluminized Ni films are ~30 μ m-thick for the five coating systems.

2.2 Microstructures of the CeO₂ free coatings after annealing

The aluminide coating is degraded by the interdiffusion between the aluminide and the underlying metallic substrate at high temperature. As shown in Fig.2a, δ -Ni₂Al₃ is fully degraded into a Ni-rich β -NiAl phase (Ni_{0.58}Al_{0.42}) in the

Table 1 Aluminide coating systems formed by partially aluminizing the electrodeposited Ni films with different CeO₂ contents and particle sizes

Coating system	Particle size	Particle content in electrodeposited Ni film/wt%
Coating-1	-	0
Coating-2	15~30 nm	1
Coating-3	15~30 nm	2
Coating-4	15~30 nm	3
Coating-5	5 μ m	1

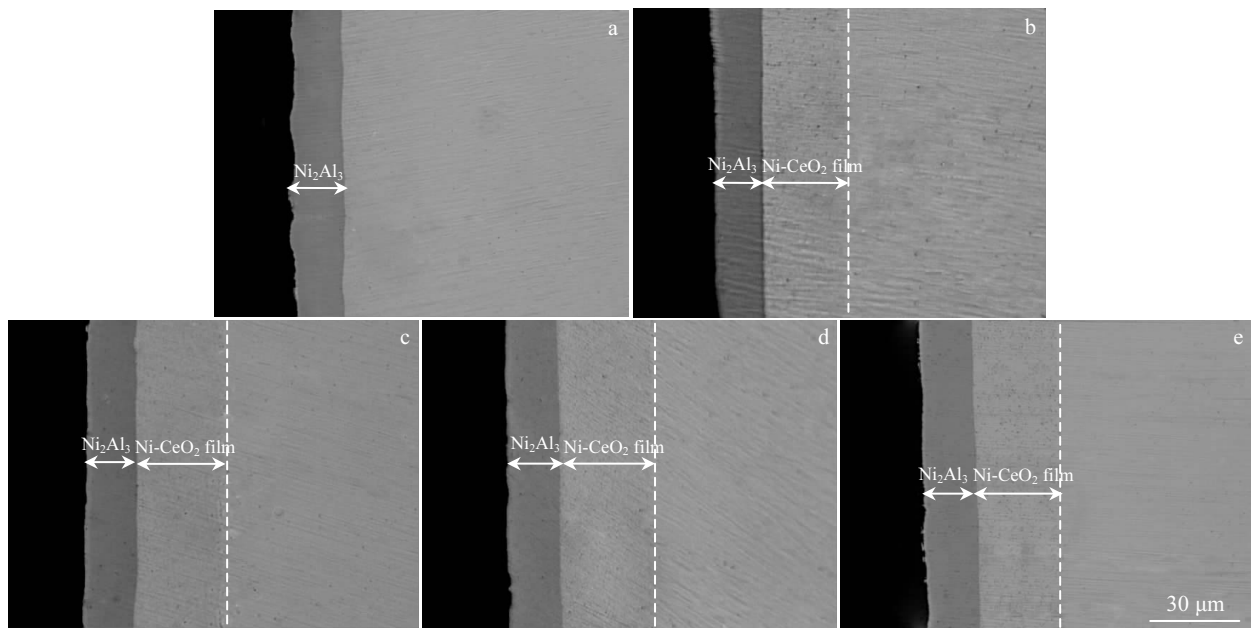


Fig.1 Cross-sectional morphologies of the δ -Ni₂Al₃ coatings formed by aluminizing Ni film (a), Ni film containing 1 wt% (b), 2 wt% (c), and 3 wt% (d) nanometer CeO₂, and Ni film containing 1 wt% micrometer CeO₂ (e)

detected area after 10 min annealing for the CeO₂-free aluminide coating system of δ -Ni₂Al₃/Ni (coating-1). Beside the Ni-rich β -NiAl, Ni₃Al is also acquired after 60 min annealing according to the XRD pattern (Fig.2b). It demonstrates that significant interdiffusion occurs between the aluminide and the Ni film. Fig.3 shows the SEM cross-sectional morphologies and EDS line scans of Al and Ni and local quantitative measurements of Al for coating-1 after 10 and 60 min annealing at 1000 °C. It reveals the composition evolution of the CeO₂-free aluminide coating with time during annealing at 1000 °C. The δ phase degradation starts from the Ni₂Al₃/Ni film interface. After 10 min annealing, the aluminide coating in its δ phase has been degraded into two

layers: an outer layer of Ni-rich β -NiAl (36.1 at% Al as arrowed) and an inner layer of Ni₃Al (26.0 at% Al as

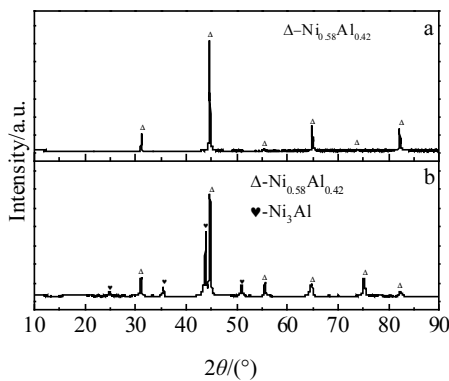


Fig.2 XRD patterns of coating-1 annealed for 10 min (a) and 60 min (b) at 1000 °C

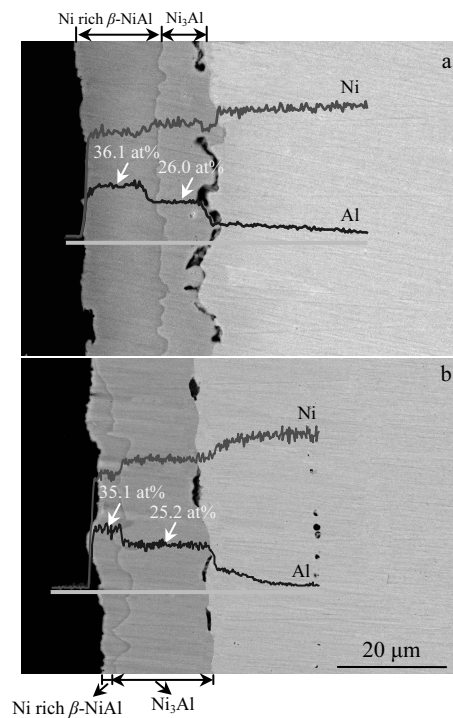


Fig.3 SEM cross-sectional morphologies and EDS line scans of Al and Ni and local quantitative measurements of Al for coating-1 after 10 min (a) and 60 min (b) annealing at 1000 °C

from the different color contrast (Fig.3a). With the increase of the annealing time, the Ni-rich β -NiAl continues to degrade into Ni_3Al from the interface of Ni-rich β -NiAl/ Ni_3Al , forming a thinner Ni-rich β -NiAl layer and a thicker Ni_3Al layer for 60 min annealing (Fig.3b).

2.3 Microstructures of the coatings with nanometer CeO_2 after annealing

For the CeO_2 -containing coating system of coating-2, δ - Ni_2Al_3 has been degraded into an Al-rich β -NiAl phase ($\text{Ni}_{0.9}\text{Al}_{1.1}$) in the probed surface layer after 10 min annealing as seen in Fig.4a. Ni rich β -NiAl phase ($\text{Ni}_{1.1}\text{Al}_{0.9}$) is detected after 60 min (Fig.4b). It reveals that the degradation of coating-2 is much slighter than that of coating-1, which could be further confirmed by the cross-sectional morphologies. The annealed aluminide coating after 10 min annealing exhibits two zones: zone I with pores and zone II with few pores according to the morphological characteristics (Fig.5a). Zone I is an Al-rich β -NiAl layer on a basis of the XRD and EDS analyses (51.5 at% Al as arrowed). Zone II is double-layered: an outer layer of Ni-rich β -NiAl (39.6 at% Al) and an inner layer of Ni_3Al (23.8 at% Al). The interdiffusion of Al and Ni between the aluminide coating and Ni film causes heavier degradation for 60 min annealing, as shown in Fig.5b. The outer Al-rich β -NiAl layer has been totally transformed into Ni-rich β -NiAl (44.1 at% Al as arrowed) and the thickness of the aluminide coating increases with time. It is believed that zone I which is as thick as the original δ - Ni_2Al_3 coating is not varied in thickness with the annealing time, while the thickness of zone II increases by $\sim 14 \mu\text{m}$ from $\sim 16 \mu\text{m}$ for 10 min annealing to $\sim 30 \mu\text{m}$ for 60 min annealing (including the increase of the thickness of the inner Ni_3Al layer from $\sim 8 \mu\text{m}$ to $\sim 13 \mu\text{m}$). From the EDS line scans in Fig.5b, the depth profiles of Al and Ni for 60 min annealing have gentler slopes compared with the results for 10 min annealing, demonstrating significant interdiffusion between the aluminide and the Ni film.

The δ phase in the probed surface zone of the coating-3 has been transformed to the Al-rich β -NiAl ($\text{Ni}_{0.9}\text{Al}_{1.1}$) for 10 min

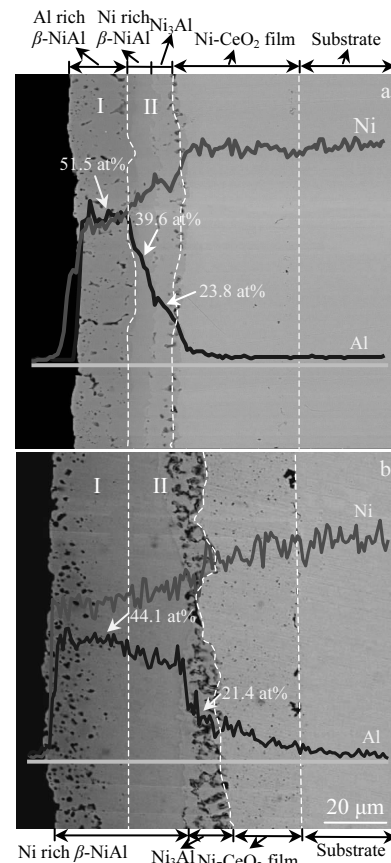


Fig.5 SEM cross-sectional morphologies and EDS line scans of Al and Ni and local quantitative measurements of Al for coating-2 after 10 min (a) and 60 min (b) annealing at 1000 °C

annealing (as shown in Fig.6a), which is similar to that of coating-2. After 60 min annealing, Ni-rich β -NiAl ($\text{Ni}_{1.04}\text{Al}_{0.96}$) forms on the basis of the XRD results (Fig.6b). Thus less interdiffusion occurs at the δ - Ni_2Al_3 /Ni film interface for coating-3 compared with that of coating-2 for 60 min annealing (Fig.4b). Fig.7a and 7b show an apparent structural evolution of

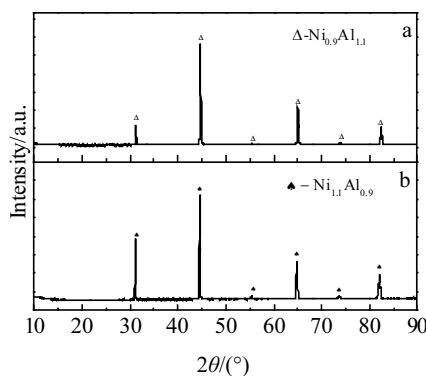


Fig.4 XRD patterns of coating-2 annealed for 10 min (a) and 60 min (b) at 1000 °C

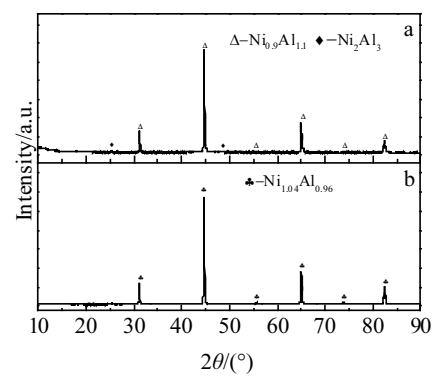


Fig.6 XRD patterns of coating-3 annealed for 10 min (a) and 60 min (b) at 1000 °C

coating-3 occurring with time during the vacuum annealing at 1000 °C. The annealed aluminide coating also exhibits two zones after 10 min at 1000 °C as that of coating-2. The thickness of zone II increases to ~ 30 μm with the expanding of the annealing time. After 60 min annealing, the Al content of Zone I (49.3 at% Al as arrowed) is more than that of coating-2 (44.1 at% Al), which is consistent with the XRD results (as shown in Fig.5b and Fig.7b).

XRD characterization indicates that the δ phase in the probed surface zone of the coating-4 has been transformed to the Al-rich β-NiAl (Ni_{0.9}Al_{1.1} as presented in Fig.8) both for 10 min annealing and 60 min annealing. The XRD results demonstrate that coating-4 performs the least degradation because of the interdiffusion between the coating and the substrate. The characteristic morphologies in Fig.9 could further confirm it. Although the XRD pattern and cross-sectional morphology of coating-4 are similar to that of coating-2 and coating-3 after annealing for 10 min, coating-4 exhibits a much narrower zone II (Fig.9a). The annealing time seems not to affect the morphologies of the two zones significantly, only the thickness of zone II increases by ~10 μm from ~8 μm for 10 min annealing to ~18 μm for 60 min annealing. Apparently, the more

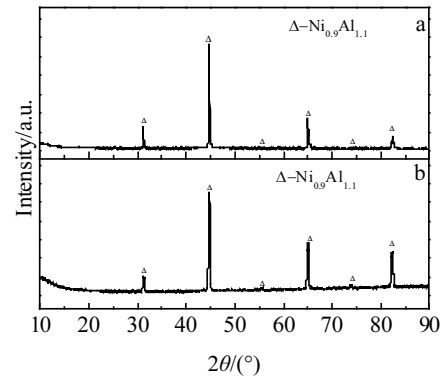


Fig.8 XRD patterns of coating-4 annealed for 10 min (a) and 60 min (b) at 1000 °C

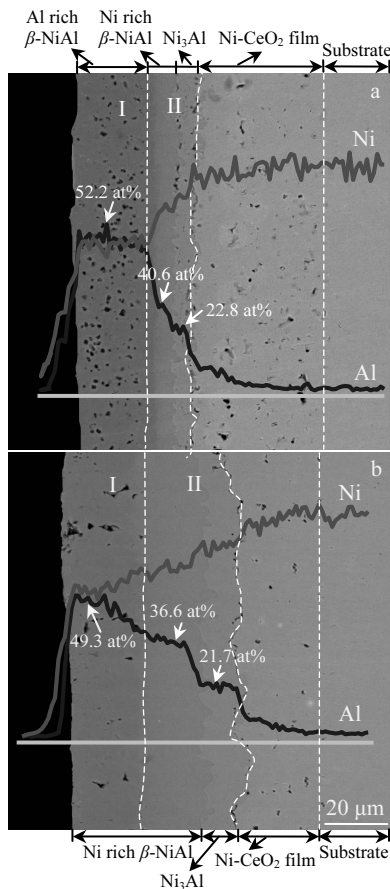


Fig.7 SEM cross-sectional morphologies and EDS line scans of Al and Ni and local quantitative measurements of Al for coating-3 after 10 min (a) and 60 min (b) annealing at 1000 °C

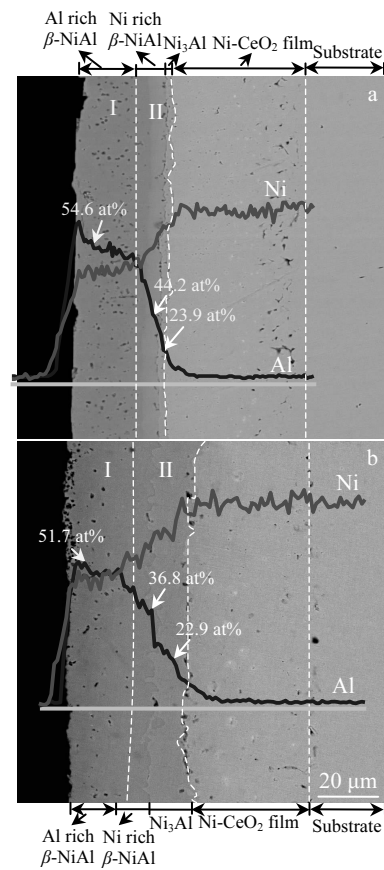


Fig.9 SEM cross-sectional morphologies and EDS line scans of Al and Ni and local quantitative measurements of Al for coating-4 after 10 min (a) and 60 min (b) annealing at 1000 °C

the thickness of zone II increases, the more severe the degradation occurs. The degradation of coating-4 is not significant for 60 min annealing with respect to that of coating-3 and coating-2. The EDS line scans in Fig.9b show that the depth profiles of Al and Ni for 60 min annealing are as sharp as those for 10 min at the degradation front of the aluminide, indicating

that the interdiffusion across the interface is not substantial.

On basis of the comparison results presented here, one can assume that the addition of CeO₂ nanoparticles could mitigate the degradation of the aluminide coating during annealing and the coating systems have better blocking effect when the particle contents increase which is 1 wt%~3 wt%. It is believed that the nanoparticles of CeO₂ could accumulate at the degradation front of the aluminide at high temperature and the formed CeO₂-rich layer acting as a diffusion barrier suppress the degradation of the aluminide coating. The mechanism for the self-formation of the CeO₂ diffusion barrier layer in the aluminide coating has been proposed, as described in the previous work^[26]. Based on the microstructures of the coatings with nanometer CeO₂ after different lengths of annealing time combined with the model proposed earlier, the degradation procession of the aluminide coating systems with different CeO₂ contents is illustrated in Fig.10. The sketch shown in Fig.10a reveals the annealing process of the coating system containing relatively high CeO₂ content (e.g. ~3 wt% as that of coating-4). When annealing starts, interdiffusion of Ni and Al occurs at the interface of δ -Ni₂Al₃ coating and the Ni film (stage I). Then β -NiAl phase firstly forms at the interface of Ni₂Al₃/Ni-CeO₂ (stage II). Accordingly, two new interfaces form which are marked with I₁ and I₂. The faster diffusion of Al with respect to Ni through I₁ leads to the counter-diffusion of Kirkendall vacancies to the surface of the coating^[27]. The vacancies condense and then form voids at sinks such as grain boundaries, impurities, the interface of CeO₂ and aluminides in this work due to the high defect density here (as presented in Zone I of Fig.5). Meanwhile, predominant Ni diffusion across I₂ induces a flux of Kirkendall vacancies which diffuse to the Ni-CeO₂ film^[28]. For a similar reason, voids form at the interface of aluminide/Ni (I₂) and near the oxides of Ni-CeO₂ film (Fig.5b). The inward diffusion of Al leads the region of NiAl phase extending into the alloy substrate, which is accompanied by the inward movement of aluminide/Ni interface. During the movement of interface, the interface would sweep the randomly dispersed CeO₂ in Ni-CeO₂ film and then drags the particles to move forward. The CeO₂ particles progressively enrich at the interface, forming the CeO₂-rich layer (stage III). When the CeO₂ content decreases (as shown in Fig.10b), fewer nanoparticles disperse in the coating system (stage I). Accordingly, fewer CeO₂ particles enrich at the degradation front (stage II) and Ni-rich β -NiAl phase at the area close to the interface of aluminide/Ni continued to be degraded into γ -Ni₃Al phase caused by further interdiffusion (stage III).

2.4 Microstructures of the coatings with micrometer CeO₂ after annealing

To understand the effect of particle sizes on the interdiffusion between the aluminide coating and substrate, the δ -Ni₂Al₃/Ni coating system containing micrometer CeO₂ particles (coating-5) is also prepared for comparison. Same as the coating system without CeO₂, aggravated interdiffusion in coating-5

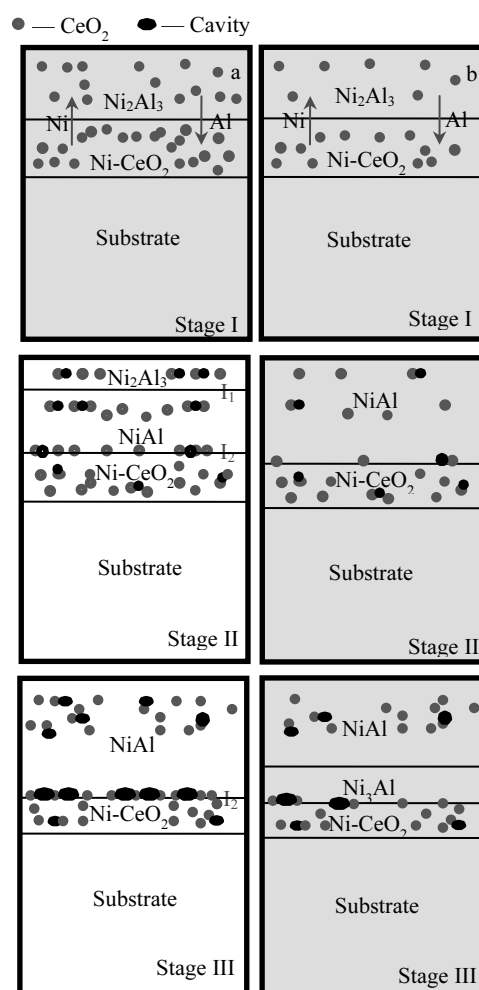


Fig.10 Schematic diagrams of degradation procession for the aluminide coating systems with relatively high nanometer CeO₂ contents (a) and relatively low nanometer CeO₂ contents (b)

leads the δ phase aluminide to be degraded into Ni-rich β -NiAl phase (Ni_{1.1}Al_{0.9}) at the area close to surface only after 10 min annealing and some peaks of Ni₃Al are also probed after 60 min annealing (as shown in Fig.2). Fig.11 shows the evolution in phase composition of the δ -Ni₂Al₃ coating with time during annealing at 1000 °C. The morphological characteristics obtained for coating-5 are similar to those of the coatings without particles. It consists of an outer layer of Ni-rich β -NiAl and an inner layer of Ni₃Al, according to the 37.3 at% and 27.6 at% Al measured on the areas as indicated in the EDS line scan (Fig.11a). Severe degradation is observed at the δ -Ni₂Al₃/Ni film interface, as revealed by the depth profiles of Al and Ni. This result indicates that the presence of micrometer CeO₂ particles has little effect on the interdiffusion between the coating and the underlying Ni film.

A particle either moves along with an individual migrating boundary if $V_{p*} \geq V_B$ (V_{p*} is the maximum migrating rate of the particle moving together with the boundary, V_B is the boundary

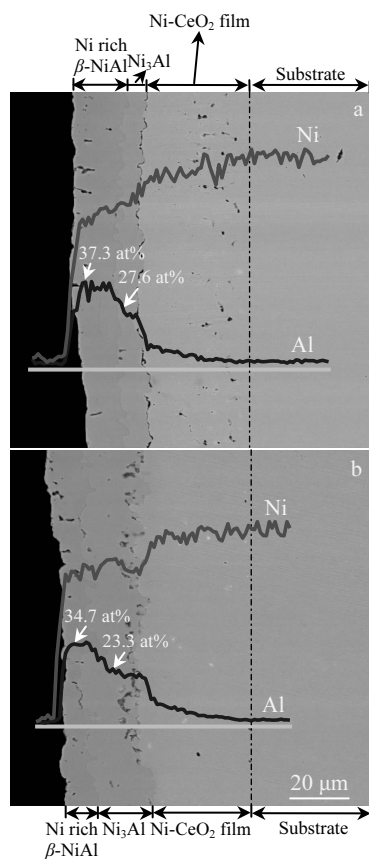


Fig.11 SEM cross-sectional morphologies and EDS line scans of Al and Ni and local quantitative measurements of Al for coating-5 after 10 min (a) and 60 min (b) annealing at 1000 °C

migrating rate) or detaches from the boundary (immovable particle) in the opposite case^[29]. The ability or inability of a particle to move along with the migrating boundary depends on both the properties of the particle and the interaction of the particle with the boundary. It is believed that a particle is able to move together with a certain boundary (the boundary energy and V_B are constant) if $r < r^*$ (r is the radius of the particle assumed spherical in shape, r^* is the maximum radius of the particle moving together with the boundary)^[30,31]. Hence, for the CeO_2 particle as small as in nanosize regime (~ 40 nm), it would be dragged by the interface with its advancement into the Ni film (Fig.10). However, when the CeO_2 particles with micron size (~ 5 μm) are added in the Ni film, the mobility of the particle is negligibly small. Consequently, the micrometer particles are immobile and cannot be dragged by the moving interface during the annealing. That's the reason that the degradation of coating-5 is much more severe than those of coating systems with CeO_2 nanoparticles.

3 Conclusions

1) The addition of nanometer CeO_2 in the coating system of

$\delta\text{-Ni}_2\text{Al}_3/\text{Ni}$ could mitigate the interdiffusion between the aluminide coating and underlying substrate during vacuum annealing at 1000 °C. The blocking effect can be significantly improved with the increase of the CeO_2 content which is 1~3 wt%. The reason could be that more CeO_2 particles enrich at the interface of the aluminide/Ni to block the interdiffusion while the content of CeO_2 in film increases.

2) The addition of micrometer CeO_2 in the coating system of $\delta\text{-Ni}_2\text{Al}_3/\text{Ni}$ has little influence on the interdiffusion between the aluminide coating and underlying substrate during vacuum annealing. It is assumed that the CeO_2 particles in micron size range could not be dragged by the interface of aluminide/Ni and accordingly the CeO_2 -rich layer could not form at the degradation front as the coating system with nanoparticles.

References

- Zhou Y H, Zhao X F, Zhao C S et al. *Corrosion Science*[J], 2017, 123: 103
- Wang X, Peng X, Tan X et al. *Scientific Reports*[J], 2016, 6: 29 593
- Liu Z J, Zhao X S, Zhou C G. *Corrosion Science*[J], 2015, 92: 148
- Sun D J, Liang C Y, Shang J L et al. *Applied Surface Science*[J], 2016, 385: 587
- Xu C, Peng X, Wang F. *Corrosion Science*[J], 2010, 52(3): 740
- Wang R L, Gong X Y, Peng H et al. *Applied Surface Science*[J], 2015, 326: 124
- Huo J J, Shi Q Y, Zheng Y R et al. *Materials Characterization*[J], 2017, 124: 73
- Peng Z R, Povstugar I, Matuszewski K et al. *Scripta Materialia*[J], 2015, 101: 44
- Tan X P, Hong H U, Choi B G et al. *Journal of Materials Science*[J], 2013, 48(3): 1085
- Matuszewski K, Rettig R, Matysiak H et al. *Acta Materialia*[J], 2015, 95: 274
- Ghasemi R, Valefi Z. *Surface and Coatings Technology*[J], 2018, 344: 359
- Bai Z M, Li D Q, Peng H et al. *Progress in Natural Science: Materials International*[J], 2012, 22(2): 146
- Narita T. *Canadian Metallurgical Quarterly*[J], 2011, 50(3): 278
- Ren P, Zhu S L, Wang F H. *Applied Surface Science*[J], 2015, 359: 420
- Al Jabbari Y S, Fehrman J, Barnes AC et al. *Coatings*[J], 2012, 2(3): 160
- Liu L T, Li Z X, Hua Y F et al. *Rare Metal Materials and Engineering*[J], 2014, 43(11): 2708 (in Chinese)
- Li H Q, Wang Q M, Jiang S M et al. *Corrosion Science*[J], 2010, 52(5): 1668
- Saremi M, Valefi Z. *Ceramics International*[J], 2014, 40(8): 13 453
- Müller J, Neuschütz D. *Vacuum*[J], 2003, 71(1-2): 247
- Müller J, Schierling M, Zimmermann E et al. *Surface and Coatings Technology*[J], 1999, 120-121: 16

- 21 Jamali H, Mozafarinia R, Razavi R S et al. *Ceramics International*[J], 2012, 38(8): 6705
- 22 Li W Z, Yi D Q, Li Y Q et al. *Journal of Alloys and Compounds*[J], 2012, 518: 86
- 23 Wang Q M, Wu Y N, Guo M H et al. *Surface and Coatings Technology*[J], 2005, 197(1): 68
- 24 Knotek O, Lugscheider E, Löffler F et al. *Surface and Coatings Technology*[J], 1994, 68-69: 22
- 25 Guo C A, Wang W, Cheng Y X et al. *Corrosion Science*[J], 2015, 94: 122
- 26 Tan X, Peng X, Wang F. *Surface and Coatings Technology*[J], 2013, 224: 62
- 27 Paul A, Kodentsov A A, van Loo F J J et al. *Journal of Alloys and Compounds*[J], 2005, 403(1-2): 147
- 28 Frank S, Divinski S V, Södervall U et al. *Acta Materialia*[J], 2001, 49(8): 1399
- 29 Novikov V Y. *Scripta Materialia*[J], 2006, 55(3): 243
- 30 Novikov V Y. *Acta Materialia*[J], 2010, 58(9): 3326
- 31 Gottstein G, Shvindlerman L S. *Acta Metallurgica et Materialia*[J], 1993, 41(11): 3267

CeO₂ 颗粒含量和尺寸对铝化物涂层和基体互扩散行为的影响

谭晓晓, 孙 丹

(上海工程技术大学, 上海 201620)

摘 要: 通过在 Ni 基体电沉积纳米 CeO₂ 颗粒 (15~30 nm) 含量~0, ~1%, ~2%, ~3% (质量分数, 下同) 和微米 CeO₂ 颗粒 (5 μm) 含量~1% 的 Ni-CeO₂ 复合镀层并对其进行部分渗铝, 制备了不同 CeO₂ 颗粒含量和尺寸掺杂的 δ-Ni₂Al₃/Ni 涂层体系。将以上 CeO₂ 掺杂的铝化物涂层在 1000 °C 真空退火不同时间, 研究 CeO₂ 颗粒含量和尺寸对铝化物涂层和基体互扩散行为的影响。退火结果表明, 纳米 CeO₂ 颗粒的添加可有效减轻 δ-Ni₂Al₃/Ni 涂层体系的退化, 而且随着 CeO₂ 颗粒含量的增加, 其对互扩散的抑制作用明显增强; 但微米 CeO₂ 颗粒的添加对涂层和基体的互扩散几乎没有影响。这是因为 CeO₂ 颗粒含量和尺寸会影响高温过程中铝化物/Ni 镀层界面处 CeO₂ 富集层的形成, 该富集层可作为扩散障, 阻碍铝化物涂层和基体的互扩散。

关键词: 铝化物涂层; 退火; 扩散障; 氧化物掺杂; 互扩散

作者简介: 谭晓晓, 女, 1988 年生, 博士, 讲师, 上海工程技术大学工程实训中心, 材料工程学院, 上海 201620, 电话: 021-67791247, E-mail: xxtan@sues.edu.cn